ADVANCES IN ATMOSPHERIC SCIENCES, VOL. 22, NO. 2, 2005, 220–229

The Shallow Meridional Overturning Circulation in the Northern Indian Ocean and Its Interannual Variability

HU Ruijin*[1] (胡瑞金), LIU Qinyu[1] (刘秦玉), WANG Qi[1] (王 启),
J. Stuart GODFREY[2], and MENG Xiangfeng[1] (孟祥凤)

[1] *Physical Oceanography Laboratory & Ocean-Atmosphere Interaction and Climate Laboratory, Ocean University of China, Qingdao* 266003

[2] *CSIRO, Division of Marine Research, GPO Box* 1538, *Hobart, Tasmania, Australia*

(Received 29 January 2004; revised 29 November 2004)

ABSTRACT

The shallow meridional overturning circulation (upper 1000 m) in the northern Indian Ocean and its interannual variability are studied, based on a global ocean circulation model (MOM2) with an integration of 10 years (1987–1996). It is shown that the shallow meridional overturning circulation has a prominent seasonal reversal characteristic. In winter, the flow is northward in the upper layer and returns southward at great depth. In summer, the deep northward inflow upwells north of the equator and returns southward in the Ekman layer. In the annual mean, the northward inflow returns through two branches: one is a southward flow in the Ekman layer, the other is a flow that sinks near 10°N and returns southward between 500 m and 1000 m. There is significant interannual variability in the shallow meridional overturning circulation, with a stronger (weaker) one in 1989 (1991) and with a period of about four years. The interannual variability of the shallow meridional overturning circulation is intimately related to that of the surface wind stress. Several indices are proposed to describe the anomaly of this circulation associated with the cross-equatorial part.

Key words: meridional overturning circulation, northern Indian Ocean, interannual variability, wind stress, circulation index

1. Introduction

Many researchers have pointed out that SST in the northern Indian Ocean affects not only the rainfall in India (Shukla and Mooley, 1987) and Australia (Nichols, 1985), but also the East Asian monsoon (Xiao and Yan, 2001), the northwestern Pacific subtropical high (Wu et al., 2000), and the summer rainfall in China (Chen, 1991; Guo et al., 2002). So more and more studies have focused on the Indian Ocean. Recently, the finding of the Indian Ocean dipole event (Saji et al., 1999), which shows that the Indian Ocean can develop an independent ENSO-like variability mechanism (Webster et al., 1999), gives rise to new interests in this region (Murtugudde and Busalacchi, 1999; Li and Mu, 2001).

The tropical Indian Ocean is unique in many aspects, compared with the tropical Pacific and/or the tropical Atlantic (Hu, 2003). One of these uniquenesses is that, as first pointed out by Levitus (1988), the annual mean wind stress in the Indian Ocean basically changes its direction from westward to eastward across the equator from the south, resulting in southward Ekman transport on both sides of the equator. The mass conservation constraint requires that the southward Ekman transport must be replaced by colder, deeper northward flow. This will cause southward net heat transport across the equator. Such a process is perhaps the most important way in setting the long-term mean net surface heat flux north of the equator in the Indian Ocean (Godfrey et al., 2001). Besides this, the annual mean wind on the equator is westerly (e.g., Schott and McCreary, 2001), which is another unique characteristic that is contrary to the easterly on the equator of the Pacific or of the Atlantic, implying that downwelling, not upwelling, occurs there. All these facts imply that the meridional overturning cell must cross the equator, which is quite

*E-mail: huruijin@ouc.edu.cn

different from the subtropical-to-tropical meridional overturning cell in the Pacific or the Atlantic (Schott and McCreary, 2001; Schott et al., 2002).

The meridional circulation plays a very important role in the heat budget, as well as the variations of SST, in the northern Indian Ocean. So these related problems are always topics of research for scientists. Many authors (e.g., Wacongne and Pacanowski, 1996; Garternicht and Schott, 1997; Lee and Marotzke, 1998) have studied the variability of the meridional overturning circulation, revealing the meridional heat transport and investigating the dynamics involved therein. But they confined their research to the seasonal timescale. Some authors (e.g., Schott et al., 2002) showed further the 3D pathway of the meridional circulation in summer, but the direct evidence they gave was inadequate. Yet these researchers paid little attention to the interannual variability of the meridional circulation. Furthermore, no one proposed an index to describe the variability of this circulation.

In this paper, we focus on the study of the interannual variability of the meridional overturning circulation of the northern Indian Ocean (north of 7°S), as well as the related dynamics, using the data of a 10-yr integration from a global ocean circulation model. As a basis, the climatology of this circulation will also be used. Since two types of meridional overturning cells, deep and shallow, exist in the Indian Ocean (Schott and McCreary, 2001; Schott et al., 2002), to avoid misunderstanding, we state that the meridional overturning circulation studied in this paper refers to the shallower one (upper 1000 m).

The structure of this paper is as follows. Section 2 gives the outline of the details of the model and its assessment. In section 3, the climatology of the shallow meridional overturning cell and its interannual variability, as well as the related dynamics, are analyzed. The paper ends with a summary.

2. The model and its assessment

2.1 *Model details*

The model is a global ocean circulation model based on the Modular Ocean Model version 2 (MOM 2) (Pacanowski, 1995; Hu, 2003). The zonal resolution is 2°, and the meridional resolution is 0.5° within 10°N –10°S, increasing poleward with 5.85° grid spacing near the poles. The vertical is divided into 25 levels with a maximum depth of 5000 m and 12 levels in the upper 185 m. The integration time step is 900 s.

The wind stress is from Florida State University (FSU) (Legler et al., 1989; Stricherz et al., 1992), with C_d=0.0015 (C_d is the drag coefficient), blended with Hellerman and Rosenstein (1983) wind stresses poleward of 30°N/S. The heat flux was parameterized using International Satellite Cloud Climatology Project (ISCCP) net solar shortwave radiation plus a flux correction (Schiller et al., 1998). The fresh water flux is restored to Levitus et al. (1994) data. The horizontal viscosity and diffusivity are 4000 m^2 s^{-1}, and the vertical viscosity and diffusivity are determined by the Chen scheme (Chen et al., 1994; Godfrey and Schiller, 1997). In the Indonesian Archipelago region, the vertical diffusivity and viscosity are increased to simulate tidal mixing there (Ffield and Gordon, 1992). Salinity is relaxed to observed values near the mouth of the Red Sea. Water transparency varies with position according to Simonot and Letreut (1986).

The model was first run for 10 years with mean seasonal wind stresses and speeds, humidity fraction and shortwave radiation, plus strong relaxation to observed SSTs. Seasonal flux corrections were calculated, and subsequent runs started from conditions at the end of this spinup run using meteorological forcing for 1985–1996 with flux corrections applied.

2.2 *Model assessment*

Before proceeding to any further, we check whether the model gives a reasonable simulation of the real Indian Ocean. A comprehensive study for comparing the results of this model with observations was made by Hu (2003), so here only the comparison of the annual mean cross equator flow of the Indian Ocean is given (Fig. 1). As shown in the figure, the flow pattern from the model is basically close to that from Simple Ocean Data Assimilation (SODA) (Carton et al., 2000) data. For example, the deep northward west boundary current and southward flow at a depth of about 50–100 m in the interior with larger magnitude in the western part are all similar. This means the model reproduces the structure of the cross equator flow well. This model also gives good simulations of SST, mixed layer depth, and horizontal ocean current, etc. (Hu, 2003), despite the relatively low resolution (figures not shown). So the results from the model are credible. In the next section, we will first analyze the climatology and interannual variability of the shallow meridional overturning cell in the northern Indian Ocean, then investigate the possible control mechanism and the links to the meridional heat transport across the equator, all based on the model's outputs.

3. Analysis

3.1 *Climatology*

The meridional overturning streamfunction is a

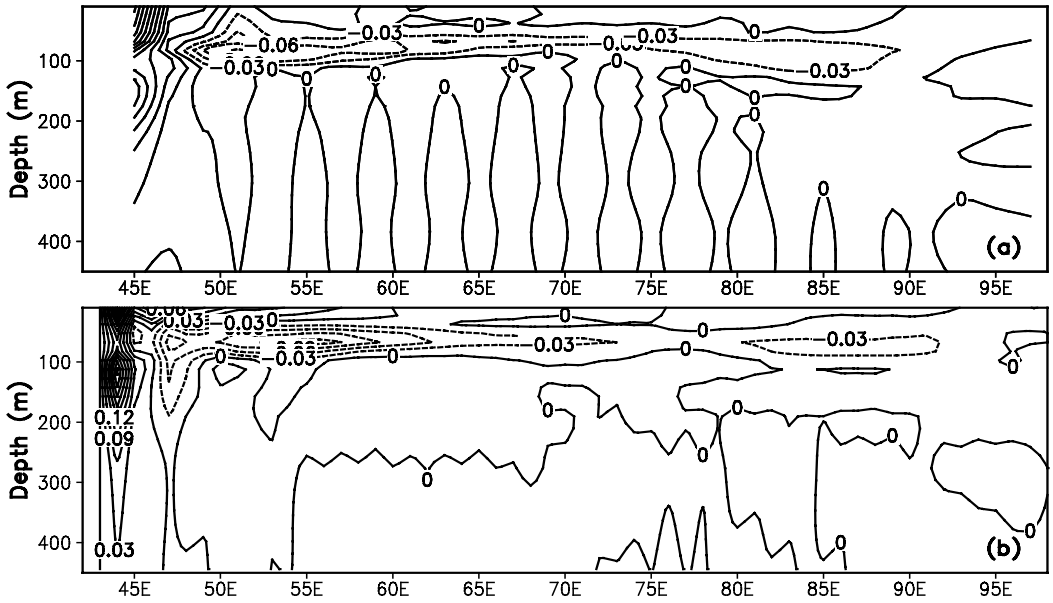

Fig. 1. Annual mean meridional velocity ($\mathrm{m\,s^{-1}}$) (northward is positive) across the equator in the Indian Ocean. (a) from the model; (b) from SODA.

useful tool to study the meridional overturning circulation in the northern Indian Ocean. It can be well defined north of 7°S (a southernmost latitude at which the northern Indian Ocean can be regarded as a half-closed basin; it is also a latitude just north of the northern tip of the entry of the Indonesian Throughflow to the Indian Ocean). To get a better understanding of the interannual variability of the meridional overturning streamfunction, its climatology needs to be described first. Figure 2 gives the results for February, August, and annual mean north of this latitude (7°S). The value in each figure at any depth and latitude represents the total mass transport to the north above this depth across this latitude, so the zonal mean flow direction can be identified.

The meridional overturning streamfunction for February (Fig. 2a) shows that the flow is northward in the upper 220 m across 7°S. For flow between 120 m and 220 m, it moves upward to about 5°S, then downwells just south of the equator and flows southward across 7°S at the depth of 420 m–700 m. McCreary et al. (1993) first identified this cell from their model and called it the tropical cell; Schott et al. (2002) also demonstrated that an upwelling zone around 5°S exists in boreal winter. For flow above 100 m, it moves northward, then downwells at about 3°S to about 50 m–100 m, then upwells near the equator and continues to move northward again, it sinks to great depth and flows southward out across 7°S at depths greater than 800 m. It is noteworthy that, in the upper 50 m near the equator, there is an anticlockwise cell with an upper branch flowing southward and a northward compensation flow beneath it. Wacongne and Paconowski (1996) first identified this cell in their model and it is now called the equatorial roll (Schott and McCreary, 2001); Miyama et al. (2003) explored the dynamics of this cell; Schott et al. (2002) verified the existence of this cell and further proved that it has little effect on the meridional heat transport due to its shallow depth.

The meridional overturning streamfunction for August (Fig. 2b) shows that the southward Ekman flow dives below the surface across the equator and continues to move across 7°S. At 7°S, there is a very deep northward compensation flow below 70 m.This flow downwells at about 7°S with depth of 200 m to 400 m. After crossing the equator, it upwells and ultimately moves southward in the Ekman layer south of 25°N. The downwelling between 10°N and 15°N at depths of 100 m to 600 m is related to the salty outflow from the Red Sea. The equatorial roll direction is opposite to that in February, with northward surface flow and southward flow beneath it. Besides these, it is noteworthy that the flow between 75 m and 250 m is always northward in both seasons, whereas the flow shallower than 75 m or deeper than 250 m experiences seasonal reversal. This is consistent with the results of Schott et al. (1990), who observed the similar characteristics in two observational surveys of the Somalia current conducted in 1984 and 1986.

The annual mean meridional overturning streamfunction (Fig. 2c) shows that three cells are apparent

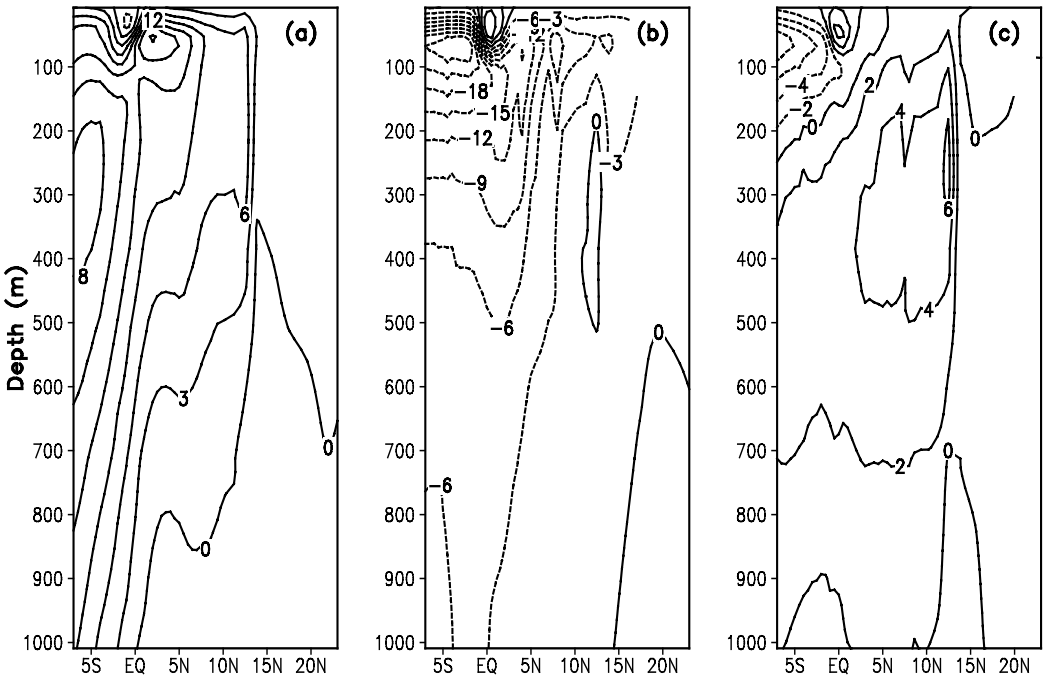

Fig. 2. Meridional overturning streamfunction (S_v=10^6 m^3 s^{-1}) of (a) February, (b) August, and (c) annual mean.

in this figure. In the first cell, flow enters the basin across 7°S between 220 m and 80 m, flows northward, apparently only to the equator, and returns southward in the Ekman layer. The second cell—referred to the "Red Sea cell" (J. S. Godfrey, personal communication, 2003)—is associated with the entrainment of dense, salty water flowing out of the Red Sea; it sinks at the mouth of the Red Sea and flows out southward across the equator between 600 m and 1000 m. The third cell is the equatorial cell mentioned above, which is quite similar with that occurring in August. It should be pointed out that the "Red Sea cell" (J. S. Godfrey, personal communication, 2003) that hardly be successfully simulated by others is consistent with observation (J. S. Godfrey, personal communication, 2003).

The climatological meridional overturning streamfunction patterns above can be explained qualitatively by the wind stress distributions. To illustrate this, Fig. 3 shows the climatological wind stress north of 20°S for February, August, and annual mean. It is obvious that, in February, the northeast monsoon is dominant in the northern Indian Ocean; this wind converges with the southeast trade wind near 10°S. In August, the trade wind across the equator turns into the southwest wind that ultimately reaches the Asian continent. The annual mean wind stress shows a similar pattern with the summer monsoon, that is, being easterly (westerly) south (north) of the equator. This implies that there is southward (northward) Ekman transport on both sides of the equator in August and the annual mean (February). This scenario is consistent with the climatological meridional overturning streamfunction (Fig. 2). As for the equatorial roll (Schott and McCreary, 2001), it is related to the meridional component of the wind stress, which is northward (southward) in August and the annual mean (February), since the Coriolis parameter is quite small near the equator.

3.2 *Interannual variability*

The northern Indian Ocean experiences large interannual variability. For brevity, only the analysis of the interannual variability of the meridional overturning streamfunction is given. Furthermore, a majority of the analyses are focused on the intercomparison between 1989 and 1991—two years which are quite different in this variable.

Figure 4 shows the meridional overturning streamfunction anomaly, for February (left panel), August (middle panel) and annual mean (right panel) in 1989. Figure 5 is the same as Fig. 4 except it shows the year 1991. In February, the biggest difference between 1989 and 1991 is that, in 1989, anomalous upwelling occurs between 3°N and 13°N from 1000 m to 300 m which then moves downwards near the equator. Besides this, in 1991, there is stronger northward (anomalous) flow below 200 m but weaker flow in the upper 100 m.

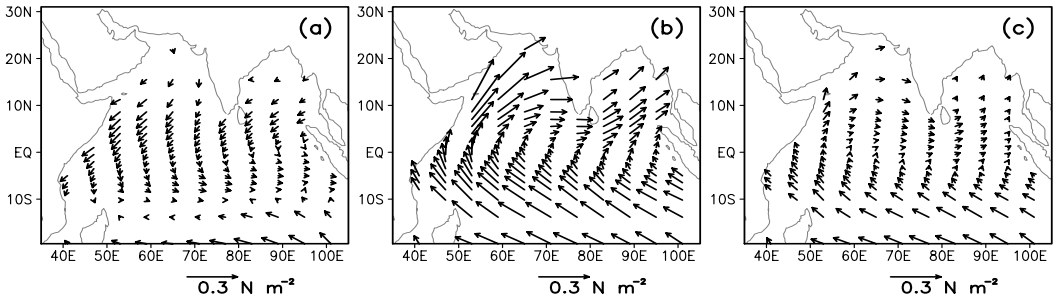

Fig. 3. Wind stress (N m^{-2}) of (a) February, (b) August, and (c) annual mean, based on FSU wind stress, for the tropical Indian Ocean.

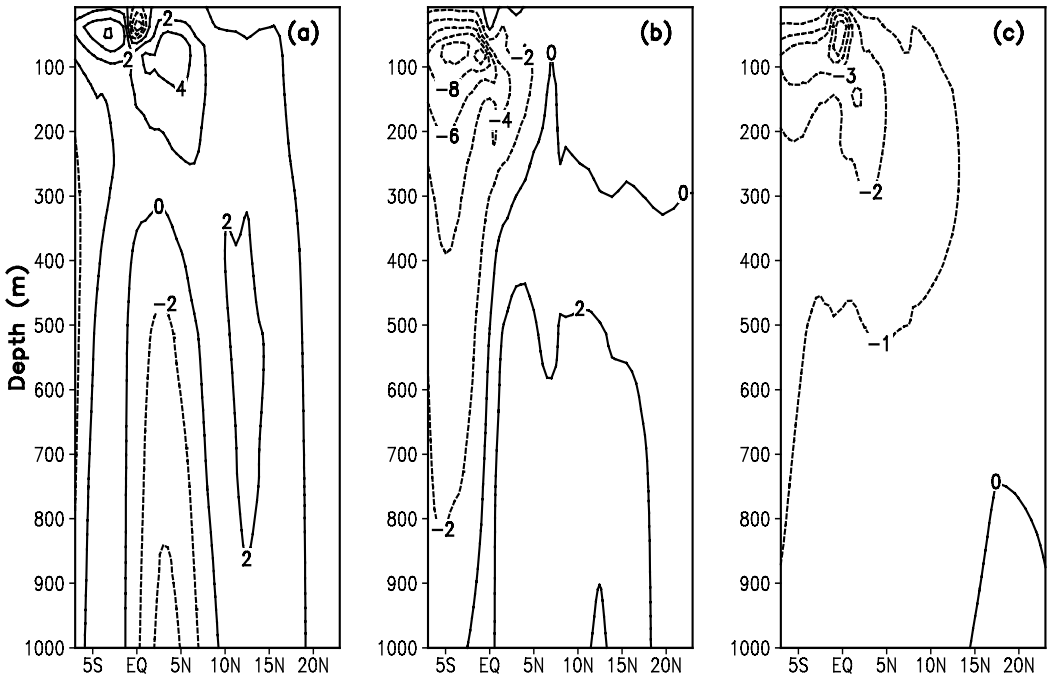

Fig. 4. Meridional overturning streamfunction anomaly (S_v) for (a) February, (b) August, and (c) annual mean of 1989.

The meridional overturning streamfunction in August shows a more obvious difference between 1989 and 1991. In August of 1989, the (anomalous) northward flow crosses 7°S below 100 m and downwells to 800 m at 5°S, then upwells to about 80 m between 0°N and 7°N, then moves southward in the Ekman layer to cross 7°S. Meanwhile, there is northward flow between 200 m and 800 m between 0°N and 18°N, which downwells at about 18°N. In August of 1991, the Ekman (anomalous) flows move northward becoming southward and downward south of 5°N. At the same time, water upwells between 5°N and 25°N at great depth. It moves southward between 100 m and 800 m, then downwells south of 2°N. The nearly opposite distribution for 1989 and 1991 is representative of the significant interannual variability in the northern Indian Ocean.

The anomalies of the annual mean meridional overturning streamfunction for 1989 and 1991 are shown in Figs. 4a and 5a, respectively. A roughly opposite distribution can be seen. In 1989, there is anomalous northward inflow below 100 m across 7°S and anomalous southward outflow above this depth. The water upwells north of 5°N and returns southward at a depth of 100 m across 7°S. In 1991, the anomalous northward Ekman flow crosses 7°S, sinks north of 5°N and returns southward across 7°S below 100 m.

The anomalous flow patterns given above indicate a stronger (weaker) shallow meridional overturning circulation in 1989 (1991), for February, August and the annual mean.

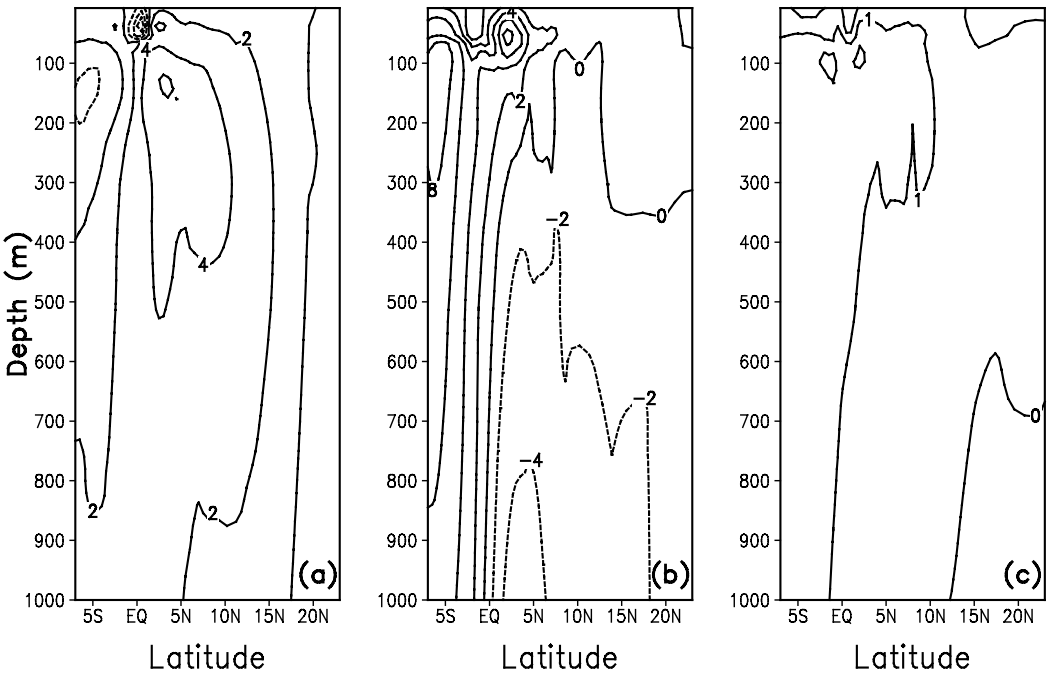

Fig. 5. Same as Fig. 4, but for the year 1991.

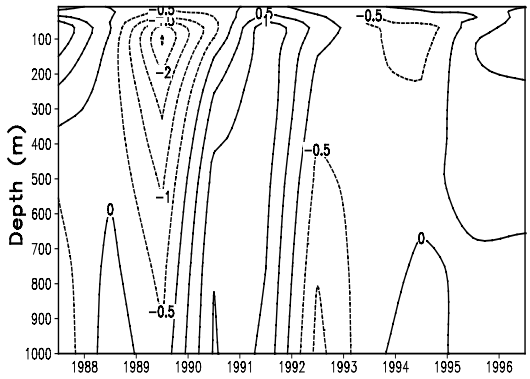

Fig. 6. Anomaly of annual mean meridional overturning streamfunction (S_v), averaged between 5°N and 5°S.

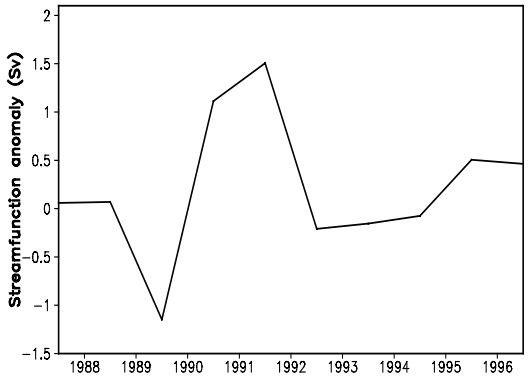

Fig. 7. Anomaly of annual mean meridional overturning streamfunction (S_v) at depth of 400 m on the equator.

To illustrate further the interannual variability of the shallow meridional circulation, the anomaly of the meridional overturning streamfunction averaged over 5°N and 5°S is calculated. For brevity, only the annual mean anomaly is shown here (Fig. 6). An interannual variability with a period of about four years can be clearly seen. Besides this, from the climatological annual mean streamfunction (Fig. 2a), we also know that the meridional circulation is stronger in 1989 than in 1991. In 1989, the meridional overturning streamfunction shows a negative anomaly in the upper 100 m and a positive anomaly below this depth, implying stronger southward flow in the upper layer and stronger northward flow in the deeper layer. The opposite phenomenon occurs in 1991, showing a weaker overturning circulation. It should be pointed out that such conclusions also hold for February and August (figures omitted).

Figure 7 shows the anomaly of the annual mean meridional overturning streamfunction at a depth of 400 m on the equator. Interannual variability with a period of about four years can also be seen. Of course, more (and longer) data is needed to confirm this period. The years 1989 and 1991 show the largest difference with negative anomaly in 1989 and positive anomaly in 1991. This can explain why we chose these two years for comparison (which can be seen from Fig. 6). The conclusions are similar for February and

August (figures omitted) and both are consistent with that of Fig. 6. Such a quantity can be regarded as an index of the variability of the shallow meridional overturning circulation in the northern Indian Ocean. It should be mentioned that the results are quite similar if the depth is taken as another value (e.g., 100 m or 200 m, figures not shown).

In the next section, we will investigate the dynamics that determines the interannual variability of the meridional overturning streamfunction.

3.3 *Control dynamics*

The region north of 7°S in the Indian Ocean can be regarded as a half-closed basin, so the total meridional mass transport across any latitude section north of this latitude (7°S) must be zero to conserve mass. The upper ocean is strongly related to Ekman transport with equal compensating flow in the opposite direction, so the meridional overturning streamfunction should be intimately related to that of the surface wind stress. This postulate was supported in the climatological case, as discussed in Section 3.1.

The relationship between the anomalous wind stress and anomalous meridional overturning streamfunction is also very clear. For brevity, only the wind anomalies for the annual means of 1989 and 1991 are given here (Fig. 8). It is evident that the wind stress anomaly is opposite in most regions north of 20°S (e.g., the band between 10°N and 10°S), implying an opposite Ekman transport (anomaly) between these two years. In 1989, a southward Ekman transport dominates, whereas in 1991 a northward one dominates. Mass conservation requires (deeper) northward inflow in 1989 and (deeper) southward outflow in 1991, leading to the opposite direction of the shallow meridional overturning circulation (anomaly) as shown in the right panels of Fig. 4 and Fig. 5. Opposite Ekman transports (anomalies) also appear in February and August when we compare 1989 with 1991 (figures not shown), which is again consistent with the patterns of the shallow meridional overturning circulation anomalies of these two months (left and middle panels in Fig. 4 and Fig. 5).

To quantitatively illustrate the relationship between the meridional circulation and wind stress, total meridional Ekman transport is calculated. Since the Ekman transport degenerates near the equator, only regions poleward of 4°N/S are involved. The result for the anomaly of the annual mean total meridional Ekman transport averaged over 5°N and 5°S displays a very obvious difference between 1989 and 1991 (figure not shown). In 1989, there is large negative Ekman transport anomaly whereas a large positive one appears in 1991, indicating a larger southward Ekman transport in the former year and a smaller one in the latter. This scenario is consistent with previous results (Figs. 6 and 7). The purpose in computing such an average (5°N and 5°S) is to get the total meridional Ekman transport across the equator indirectly. This can also explain why we calculate a two-band mean (5°N and 5°S) of the meridional overturning streamfunction anomaly as shown in Fig. 6. The largest discrepancy between the Ekman transport anomaly and the meridional overturning streamfunction anomaly (Fig. 7) occurs in 1994, a year of an identified dipole event in the tropical Indian Ocean (Saji et al., 1999). The cause needs to be further explored. A possible reason is that the streamfunction at a depth of 400 m on the equator (Fig. 7) actually indicates the strength of the cross-equatorial part of the shallow meridional overturning circulation, whereas the total meridional Ekman transport in 1994 mentioned above reflects the non-cross-equatorial meridional overturning circulation in that year. It is well known that a strong easterly appears on the equator of the eastern Indian Ocean in 1994, which means strong upwelling exists on the equator as in the Pacific or Atlantic. This equatorial upwelling forms the non-cross-equatorial cell—referred to as the eastern branch of the Subtropical Cell (Miyama et al., 2003) of the Indian Ocean. If we take the streamfunction at a depth of 70 m at 5°S (or 7°S) and the total meridional Ekman transport across this latitude as two indices to represent the strength of this subtropical cell, then we can see that such indices show exactly the same variability pattern (figures not shown). So in all, the tight relationship between the meridional overturning streamfunction and wind stress is without doubt, that is, the interannual variability of the shallow meridional circulation is mainly determined by that of the surface wind stress. This is also true for the climatological case.

3.4 *Significance in climate*

One of the uniquenesses of the northern Indian Ocean is the existence of a strong meridional heat transport variation associated with the seasonal reversal of the monsoon. Loschnigg and Webster (2000) pointed out that the amplitude of the SST variability is much smaller than the one determined by net surface heat flux alone, implying the important role of meridional heat transport on the heat budget and SST in the northern Indian Ocean, which was also demonstrated by Godfrey et al. (1995, 2001).

The meridional heat transport Q across the equator is calculated by

$$Q = \rho c_p \int_{X_w}^{X_e} \int_{-H}^{0} (VT)_{0^\circ N} dx dz$$

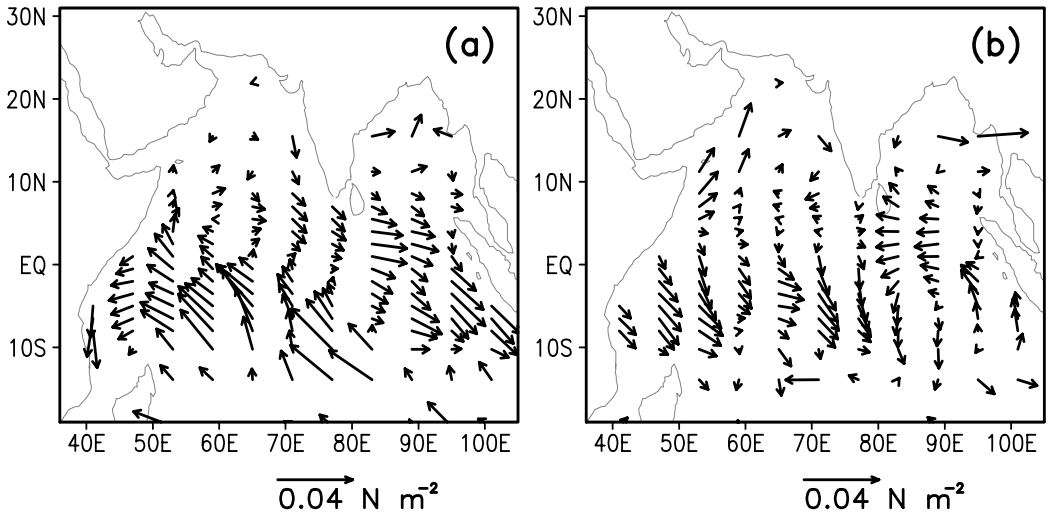

Fig. 8. Anomaly of annual mean wind stress (N m^{-2}) for (a) 1989 and (b) 1991.

Fig. 9. Anomaly of annual mean meridional heat transport (PW) across the equator (dashed) and time rate of annual mean temperature averaged over north of the equator in the Indian Ocean (units: $^{\circ}$C yr^{-1}) (solid).

where ρ and c_p are the density and heat capacity of sea water, V and T the meridional velocity and potential temperature, $X_{\rm w}$ and $X_{\rm e}$ are related to the western and eastern boundary on the equator of the Indian Ocean, and H is the depth of the ocean.

The dashed line in Fig. 9 shows the anomaly of annual mean meridional heat transport across the equator (Q). A period of roughly four years can also be seen. In 1989, there is a negative anomaly of heat transport with a value of about –0.15 PW (1 PW= 10^{15} W), whereas in 1991, the anomaly is opposite with a value of about 0.12 PW. This means more (less) heat is transported southward across the equator in 1989 (1991) since the annual mean meridional heat transport across the equator is about –0.125 PW (southward). Interestingly, the anomaly of heat transport in 1994, a dipole year in the tropical Indian Ocean (Saji et al., 1999), is quite small which is contrary to the quite large anomaly of Ekman transport (figure not shown). It should be pointed out that the value does not show marked change if the depth of integration is chosen at an intermediate level (about 1000 m) instead of H (figures not shown), implying the importance of the upper ocean in the variation of the total heat transport.

The solid line in Fig. 9 shows the time rate of annual mean SST averaged over the area north of the equator in the Indian Ocean. It is obvious that the distribution of the extremum in this figure is quite close to that in Fig. 7 or the dashed line in Fig. 9, indicating that the variability of the shallow meridional overturning circulation is closely related to the variation of SST in the northern Indian Ocean. This can explain again why we chose years 1989 and 1991 for comparison. The larger discrepancy in 1987/1988 may be due to the short integration time from the start.

Again for brevity, the analysis of February or August is omitted here.

The purpose in calculating meridional heat transport across the equator is not to investigate its dynamics (e.g., Fanning and Weaver, 1997) but to emphasize its importance in the climate of the northern Indian Ocean (e.g., Hu, 2003). It is more important that the similarity between the two lines in Fig. 9 and Fig. 7 implies that the anomaly of meridional heat transport across the equator and the time rate of SST averaged over north of the equator can be regarded as two other indices that describe the interannual variability of the shallow meridional circulation (its cross-equatorial part) in the northern Indian Ocean, besides the one defined in section 3.2. Another candidate for

the index would be related to the wind stress, but we would need to elaborate on the choice. Obviously, the advantage of the indices associated with SST (wind) is that they are convenient for practical use.

A detailed analysis of the dynamics of the meridional heat transport and its role in the heat budget will appear in another paper.

4. Summary

The shallow meridional overturning circulation in the northern Indian Ocean and its interannual variability are studied using the output from an ocean global circulation model that gives good simulations of the real Indian Ocean. The main results are as follows:

(1) The shallow meridional overturning circulation shows a prominent seasonal reversal characteristic. In winter (February), the flow is northward in the upper layer, it sinks in the Indian Ocean north of the equator and returns southward at great depth. In summer (August), the northward inflow at great depth upwells north of the equator and returns southward in the Ekman layer. In the annual mean, the northward inflow (across 7°S) returns by two branches, one upwells and returns southward in the Ekman layer, the other sinks near 10°N and returns southward at great depth (and is called the "Red Sea cell"). An equatorial roll, confined near the equator and within the mixed layer depth, with a direction opposite to the Ekman transport, can be seen in all cases.

(2) There is significant interannual variability in the shallow meridional overturning circulation. The anomalous flow patterns indicate a stronger (weaker) shallow meridional overturning circulation in 1989 (1991), in February, August and the annual mean. Besides this, a variability with a period of about four years seems to exist.

(3) The interannual variability in the shallow meridional overturning circulation is intimately related to the interannual variability in surface wind stress.

(4) Several indices that can be used to describe the interannual variability of the shallow meridional circulation associated with the cross-equatorial part are proposed. One is the meridional overturning streamfunction at a depth of 400 m on the equator; the second is the meridional heat transport across the equator; the third is the time rate of SST averaged over north of the equator. Considering both the accuracy and the convenience of use, we recommend the first one, i.e., the meridional overturning streamfunction at a depth of 400 m on the equator, as the best index.

It should be pointed out that there are many unresolved questions regarding the shallow meridional circulation in the Indian Ocean. For example, the three dimensional pathways of this circulation and its variability, as well as the dynamics involved, need to be investigated in detail.

Acknowledgments. The authors wish to thank Y. L. Zhang, A. Schiller and R. Fiedler for their tremendous amount of work in ocean modeling. We also thank the two anonymous reviewers for their helpful comments. This study was supported by National Natural Science Foundation of China (NSFC) under Grant No. 40233033.

REFERENCES

Carton, J. A., G. Chepurin, and X. Cao, 2000: A simple ocean data assimilation analysis of the global upper ocean 1950-95. Part II: Results. *J. Phys. Oceanogr.*, **30**, 311–326.

Chen, D., L. M. Rothstein, and A. J. Busalacchi, 1994: A hybrid vertical mixed-layer scheme and its application to tropical ocean models. *J. Phys. Oceanogr.*, **24**, 2156–2179.

Chen Lieting, 1991: Effect on zonal difference of sea surface temperature anomalies in the Arabian Sea and the South China Sea on summer rainfall over the Yangtze River. *Scientia Atmospheric Sinica,* **15**(1), 33–42. (in Chinese)

Fanning, A. F., and A. J. Weaver, 1997: A horizontal resolution and parameter sensitivity study of heat transport in an idealized coupled climate model. *J. Climate,* **10**, 2469–2478.

Ffield, A., and A. L. Gordon, 1992: Vertical mixing in the Indonesian thermocline. *J. Phys. Oceanogr.*, **22**, 184–195.

Garternicht, U., and F. Schott, 1997: Heat fluxes of the Indian Ocean from a global eddy-resolving model. *J. Geophys. Res.*, **102**, 21147–21159.

Godfrey, J. S., and Coauthors, 1995: The role of the Indian Ocean in the global climate system: Recommendations regarding the global ocean observing system. Report of the Ocean Observing System Development Panel, Texas A & M University, College Station, TX, USA, 89pp.

Godfrey, J. S., and A. Schiller, 1997: Tests of mixed-layer schemes and surface boundary conditions in an ocean general circulation model, using the IMET data set. CSIRO Marine Laboratories Report, 321pp.

Godfrey, J. S., G. C. Johnson, M. J. McPhaden, G. Reverdin, and S. Wijffels, 2001: The tropical ocean circulation. *Ocean Circulation and Climate*, Vol. 77, G. Siedler, J. Church, and W. J. Gould, Eds., Academic Press, 215–246.

Guo Yufu, Zhao Yan, and Wang Jia, 2002: Numerical simulation of the relationships between the 1998 Yangtze River valley floods and SST anomalies. *Adv. Atmos. Sci.*, **19**(3), 391–404.

Hellerman, S., and M. Rosenstein, 1983: Normal monthly wind stress over the world ocean with error estimates. *J. Phys. Oceanogr.*, **13**, 1093–1104.

Hu Ruijin, 2003: Study on the heat budget and the meridional circulation of the tropical Indian Ocean. Ph. D. dissertation, Ocean University of China, 99pp. (in Chinese)

Lee, C. M., and J. Marotzke, 1998: Seasonal cycle of meridional overturning and heat transport of the Indian Ocean. *J. Phys. Oceanogr.*, **28**, 923–943.

Legler, D. M., I. M. Navon, and J. J. O'Brien, 1989: Objective analysis of pseudostress over the Indian Ocean using a direct-minimization approach. *Mon. Wea. Rev.*, **117**, 709–720.

Levitus, S., 1988: Ekman volume fluxes for the world ocean and individual basins. *J. Phys. Oceanogr.*, **18**, 271–279.

Levitus, S., R. Burgett, and T. P. Boyer, 1994: *World Ocean Atlas 1994: Salinity. NOAA Atlas NESDIS 3*, Volume 3, U. S. Department of Commerce, Washington D. C., 99pp.

Li Chongyin, and Mu Mingquan, 2001: The dipole in the equatorial Indian Ocean and its impacts on climate. *Chinese J. Atmos. Sci.*, **25**(4), 433–443. (in Chinese)

Loschnigg, J., and P. J. Webster, 2000: A coupled ocean-atmosphere system of SST modulation for the Indian Ocean. *J. Climate*, **13**, 3342–3360.

McCreary, J. P., P. K. Kundu, and R. L. Molinari, 1993: A numerical investigation of dynamics, thermodynamics and mixed-layer processes in the Indian Ocean. *Progress in Oceanography*, **31**, 181–244.

Miyama, T., J. P. McCreary, T. G. Jensen, J. Loschnigg, J. S. Godfrey, and A. Ishida, 2003: Structure and dynamics of the Indian Ocean cross-equatorial cell. *Deep-Sea Res.* **50**, 2023–2048.

Murtugudde, R., and A. J. Busalacchi, 1999: Interannual variability of the dynamics and thermodynamics of the tropical Indian Ocean. *J. Climate*, **12**, 2300–2326.

Nicholls, N, 1985: Sea surface temperature and Australia winter rainfall. *J. Climate*, **2**, 965–973.

Pacanowski, R. C., 1995: MOM2 Documentation User's Guide and Reference Manual Version 1.0. GFDL Ocean Technical Report No. 3, Princeton, 232pp.

Saji, N. H., B. N. Goswami, P. N. Vinayachandran, and T. Yamagata, 1999: A dipole in the tropical Indian Ocean. *Nature*, **401**, 360–363.

Schiller, A., J. S. Godfrey, P. C. McIntosh, G. Meyers, and S. E. Wijffels, 1998: Seasonal near-surface dynamics and thermodynamics of the Indian Ocean and the Indonesian Throughflow in a global ocean general circulation model. *J. Phys. Oceanogr.*, **28**, 2288–2312.

Schott, F., M. Dengler, and R. Schoenefeldt, 2002: The shallow overturning circulation of the Indian Ocean. *Progress in Oceanography*, **53**, 57–103.

Schott, F., and J. P. McCreary, 2001: The monsoon circulation of the Indian Ocean. *Progress in Oceanography*, **51**, 1–123.

Schott, F., J. C. Swallow, and M. Fieux, 1990: The Somali Current at the equator: Annual cycle of currents and transports in the upper 1000 m and connection to neighboring latitudes. *Deep-Sea Res.* **37**, 1825–1848.

Shukla, J., and D. A. Mooley, 1987: Empirical prediction of the summer monsoon rainfall over India. *Mon. Wea. Rev.*, **115**, 695–703.

Simonot, J. Y., and H. L. Letreut, 1986: A climatological field of mean optical properties of the world ocean. *J. Geophys. Res.*, **91**, 6642–6646.

Stricherz, J., J. J. O'Brien, and D. Legler, 1992: *Atlas of Florida State University Tropical Pacific Winds for TOGA 1966–1985*. Florida State University, 256pp.

Wacongne, S., and R. Pacanowski, 1996: Seasonal heat transport in a primitive equations model of the tropical Indian Ocean. *J. Phys. Oceanogr.* **26**, 2666–2699.

Webster, P. J., A. M. Moore, J. P. Loschnigg, and R. R. Leben, 1999: Coupled ocean-atmosphere dynamics in the Indian Ocean during 1997–98. *Nature*, **401**, 356–359.

Wu Guoxiong, Liu Ping, Liu Yimin, and Li Jianping, 2000: Impacts of the sea surface temperature anomaly in the Indian Ocean on the subtropical anticyclone over the western Pacific—Two-stage thermal adaptation in the atmosphere. *Acta Meteorologica Sinica*, **58**(5), 513–522. (in Chinese)

Xiao Ziniu, and Yan Hongming, 2001: A numerical simulation of the Indian Ocean SSTA influence on the early summer precipitation of the South China during an El Niño year. *Chinese J. Atmos. Sci.*, **25** (2), 173–183. (in Chinese)